2017. September 30.

Final report on "Preparation and chemical characterisation of metal complexes for theranostic applications" (K 109029)

The project was conducted by a "four generation" research group (named "Rare(earth)metal research group") consisting of 2 emeritus professors, 3 very active young scientists close to age 40, 3-4 PhD students, several talented MSc and BSc students and 2 good technicians. The success of our work can be documented primarily by 26 publications mostly published in top ranked chemistry journals and 1 patent application. Additionally, several team members enjoyed progress in their careers: two successful habilitations, two defended PhD theses, BSc and MSc diplomas, three new PhD positions, postdoc invitations, good job offers etc. can (partly) be attributed to this project.
The Chemistry Department of the University of Debrecen has a large-scale project (GINOP-2.3.2-15-2016-00008), our group plays active role in the "Coordination Chemistry" sub-project and gets support. The project was carried out in very intensive international cooperation (France, Germany, Italy, Portugal, Spain, Sweden in COST actions and USA). These frameworks helped us in many ways including high level knowledge, indirect human resources and financial support.

Summary

We synthesised new manganese(II), copper(II), lanthanide(III), aluminium(III), gallium(III) and thallium(III) complexes with rigidified organic ligands. Detailed physico-chemical characterisation shows that some of the compounds have better thermodynamic stability, inertness and effectiveness compared to metal complexes routinely used in different modalities of medical imaging (e.g. **M**agnetic **R**esonance **I**maging, **P**ositron **E**mission **T**omography) or theragnostics (combination of diagnosis and therapy). The rigidity of the ligands was tuned by systematic substitution of open chain and macrocyclic aminocarboxylate ligands both in the backbone/macrocycle and at the pendant arms of the molecules. The complexes are ready for further studies *in vivo*, one family of Mn(II)-ethylene-diamine-tetraacetic-acid-bis(amide) derivatives was patented and earned industrial interest.

The detailed final report follows the structure of the research plan in the proposal. The published results are shown via the titles of the papers and the somewhat shortened abstracts in *Italics*, while the unpublished part is printed with normal characters.

Objectives

Motto: Tuning inertness of the complexes via rigidity of ligands is the common working idea in our sub-projects, i.e. this strategy is used throughout in our working plan.

1. Designing ligands for Mn^{2+} complexation: *tuning the thermodynamic, kinetic (dissociation and water exchange rate) parameters of Mn^{2+} complexes by careful ligand design.*

Both open chain and macrocyclic ligands can be modified by proper substitution on the backbone and/or on the pendant arms making the ligand more rigid. The effect of this fine-tuning on stability and kinetic properties has been tested on several metal-complexes of different imaging modalities, like MRI (Ln(III), Mn(II)), PET (Ga, Cu, Sc) and SPECT (In). These results might be transferred among the different modalities and/or are very useful for ligand design.
The Mn-complexes should fulfil the **general requiremenst: high stability, resistance against oxidation by air, good kinetic inertness, good relaxivity** through a labile water molecule in the inner sphere of Mn(II) having coordination number 6-7. Ligands with 6 donor atoms of rigid open chain ligands, and 12-membered macrocycles with suitable (potentially also rigid) pendant arms are the promising platforms, the fine-tuning focuses on the quality of the donor atoms and geometry of the molecules. Detailed physico-chemical characterisation of the above-mentioned behaviours together with the study of structure and formation kinetics are needed to decide if a new complex is suitable for further studies in vivo.

1.1. Mn(II) complexes with open chain ligands

1.1.1. ***New substituted ethylene-diamine-tetraacetic-acid-bis(amide) derivatives and use thereof as ligand containing Mn (II) of MRI contrast agent.*** *(Patent registration number: WO2016135523)*
The newly prepared open chain ligands for Mn(II)-complexation are the bis-amide derivatives of CDTA (trans-1,2-Diaminocyclohexane-N,N,N′,N′-tetraacetic acid), including the bis-amide piperide derivative (shown below). The Italian BRACCO Imaging Ltd. showed interest in the patent and to start joint research on this project. The contracted project is in progress.

1.1.2. Equilibrium, kinetics and relaxation properties of Mn(PhDTA) complex, conference abstract, KKK Siófok, 2014 May

The Mn(II) complex of the rigidified **PhDTA** ligand shows lower stability and better inertness compared to the Mn(CDTA) complex. (A full paper is under submission to the New Journal of Chemistry.)

1.1.3. ***cis-IPDTA: An original polyaminopolycarboxylic chelating agent from isophoronediamine. Synthesis and thermodynamic characterization of metal complexes*** in *Polyhedron*, **2016**, *109*, 115–119.; http://dx.doi.org/10.1016/j.poly.2016.02.010

An original diaminotetracarboxylic acid chelating agent (cis-IPDTA, cis-isophoronediamine-N,N,N',N'-tetraacetic acid) was prepared starting from commercially available isophoronediamine. Its protonation constants and the stability of selected metal complexes (including Mn(II) and Ln(III)) were determined by potentiometric titrations. The coordination behavior of cis-IPDTA was compared with that of the linear congener BDTA and iminodiacetic derivatives.

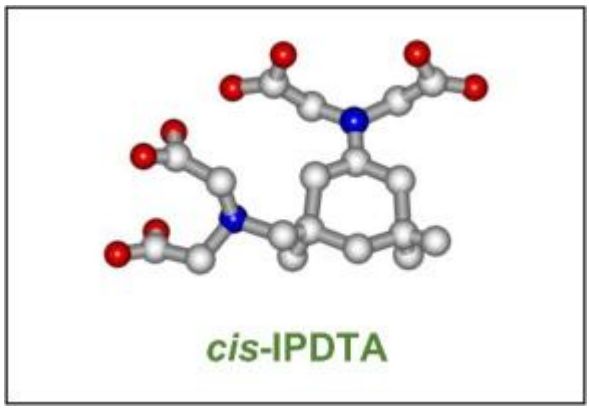

1.2. Mn(II)- macrocycle ligand systems

1.2.1. ***Picolinate-containing macrocyclic Mn^{2+} complexes as potential MRI contrast agents*** **in** *Inorg. Chem.*, **2014**, 5136-5149.; http://dx.doi.org/10.1021/ic500231z

The synthesis of the ligand Hnompa (6-((1,4,7-triazacyclononan-1-yl)methyl)picolinic acid) and a detailed characterization of the Mn^{2+} complexes formed by this ligand and the related ligands Hdompa (6-((1,4,7,10-tetraazacyclododecan-1-yl)methyl)picolinic acid) and Htempa (6-((1,4,8,11-tetraazacyclotetradecan-1-yl)methyl)- picolinic acid) are reported. These ligands form thermodynamically stable complexes in aqueous solution. The dissociation kinetics of these Mn^{2+} complexes at about neutral pH follow a spontaneous dissociation mechanism. The Mn^{2+} ion is six-coordinate in solution by the pentadentate ligand and one innersphere water molecule. The analysis of the ^{1}H NMRD and ^{17}O NMR data provides a very high water exchange rate ($k_{ex}^{298}=2.8\times10^{9}\ s^{-1}$) and an unusually high value of the ^{17}O hyperfine coupling constant of the coordinated water molecule ($A_O/\hbar=73.3\pm0.6$ rad s^{-1}). DFT calculations performed on the $[Mn(nompa)(H_2O)]^{+}\cdot2H_2O$ system (TPSSh model) provide a $A_O/\hbar$ value in excellent agreement with the one obtained experimentally.

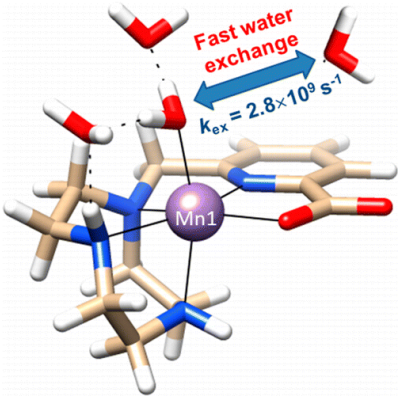

1.2.2. ***Solution thermodynamics, computational and relaxometric studies of ditopic DO3A-based Mn(II) complexes*** in *New J. Chem.*, **2015**, *39*, 539-547, http://dx.doi.org/10.1039/C4NJ01571A

Two novel ditopic DO3A-based ligands were designed and synthesized and their Mn(II)- complexes evaluated. The stability of these complexes was assessed, while modelling was adopted to gain the structural features. A detailed relaxometric characterization provided a picture of the paramagnetic properties of these dinuclear chelates, paving the way for the Mn(II)-based multimeric MRI contrast agents.

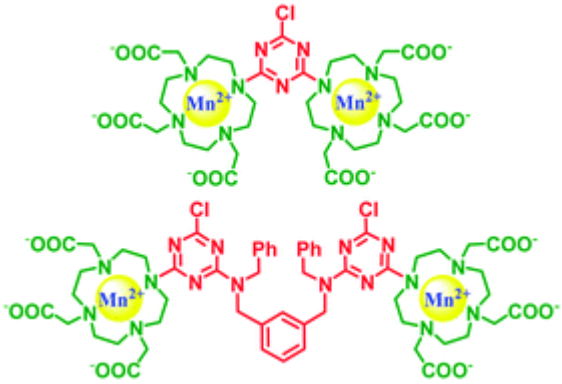

1.2.3. ***Stable Mn^{2+}, Cu^{2+} and Ln^{3+} complexes with cyclen-based ligands functionalized with picolinate pendant arms*** in *Dalton Trans.*, **2015**, *44*, 5017-5031.; http://dx.doi.org/10.1039/C4DT02985B

The complexes of metal ions of biomedical importance (Mn^{2+}, Cu^{2+} and Gd^{3+}) with octadentate ligands based on a cyclen platform incorporating two picolinate pendant arms ($dodpa^{2-}$ and $Medodpa^{2-}$) have been studied. The stability constants of the complexes do not differ, which indicates that the steric hindrance brought by the methyl groups has no significant effect on the stability. However, the stability of the [Cu(dodpa)] and [Cu(Medodpa)] complexes agrees well with the stability constant of $[Cu(dompa)]^{+}$, in line with the hexadentate coordination around the metal ion observed in

the X-ray structure of [Cu(Medodpa)]. The [Gd(dodpa)]$^{+}$ and [Gd(Medodpa)]$^{+}$ complexes display a fairly high kinetic inertness.

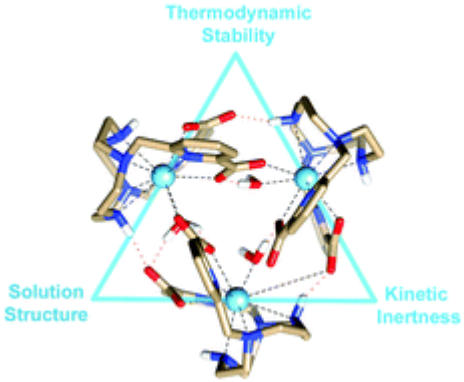

1.2.4. ***A Bisamide Derivative of [Mn(1,4-DO2A)] – Solution Thermodynamic, Kinetic, and NMR Relaxometric Studies*** in *Eur. J. Inorg. Chem.*, **2016**, 1165-1174.; http://dx.doi.org/10.1002/ejic.201501415

A new 1,4-DO2A-bisamide ligand was synthesized, and its Mn^{II} complex was prepared and investigated in detail. The stability constant of [Mn(1,4-DO2AM)]$^{2+}$ (logK_{MnL}=12.64) is 2.5 log K units lower than that of [Mn(1,4-DO2A)], its kinetic inertness is much higher. The longer rotational correlation time (τ_R=53 ps) for [Mn(1,4-DO2AM)]$^{2+}$ is mainly responsible for the slightly higher (+20 %) relaxivity (r_1=2.5 mM^{-1} s^{-1}, 20 MHz, 25 °C) with respect to that of [Mn(1,4-DO2A)]. The water exchange rate of the coordinated water molecule is one order of magnitude slower than that of [Mn(1,4-DO2A)] ($^{298}k_{ex}$=(115±6)×10^{6} s^{-1}).

1.2.5. ***Physico-chemical properties of Mn(II) complexes formed with cis- and trans-DO2A: Thermodynamic, electrochemical and kinetic studies*** in *J. Inorg. Biochem.*, **2016**, *163*, 206-213.; https://doi.org/10.1016/j.jinorgbio.2016.07.018

Equilibrium and kinetic studies were performed with Mn^{II} complexes of 1,4,7,10-tetraazacyclododecane-1,4-diacetic acid (1,4-DO2A or cis-DO2A) and 1,4,7,10-tetraazacyclododecane-1,7-diacetic acid (1,7-DO2A or trans-DO2A). The stability constants of [Mn(cis-DO2A)] are slightly higher than that of [Mn(trans-DO2A)] (logK_{MnL} = 15.68 and 15.22, respectively). Cyclic voltammetric (CV) experiments performed on [Mn(cis-DO2A)] and [Mn(trans-DO2A)] revealed quasireversible systems. The Mn^{II} ion in these complexes is more stabilized against the oxidation than in [Mn(EDTA)]$^{2-}$. The kinetic inertness of the complexes has been studied in transmetallation reactions with Cu^{II} or Zn^{II} ions. Both Mn^{II} complexes primarily undergo acid catalyzed dissociation and positions of the acetate pendant arms do not influence kinetic inertness. The kinetic inertness of these complexes is comparable to that of [Mn(NOTA)]$^{-}$ and significantly

lower than that of $[Mn(DOTA)]^{2-}$. *This complex a promising platform for the development of more efficient* Mn^{II} *complexes as alternatives to Gd-based MRI agents.*

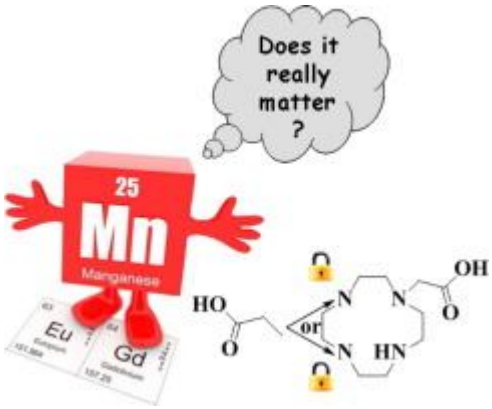

2. Describing the halide-binding as mixed ligand complex formation

2.1. Mixed complexes with the "soft" Tl(III) center

2.1.1. ***[Tl^{III}(DOTA)]⁻: An extraordinary robust macrocyclic complex*** in *Inorg. Chem.*, **2015**, *54*, 5426-5437.; https://doi.org/10.1021/acs.inorgchem.5b00458

The X-ray structure of $\{C(NH_2)_3\}[Tl(dota)]\cdot H_2O$ *shows that the* Tl^{3+} *ion is deeply buried in the macrocyclic cavity of the* $dota^{4-}$ *ligand (1,4,7,10-tetraazacyclododecane-1,4,7,10-tetraacetate). The metal ion is directly coordinated to the eight donor atoms of the ligand, which results in a twisted square antiprismatic (TSAP') coordination around* Tl^{3+}. *A multinuclear* ^{1}H, ^{13}C, *and* ^{205}Tl *NMR study combined with DFT calculations confirmed the TSAP' structure of the complex in aqueous solution, which exists as the Λ(λλλλ)/Δ(δδδδ) enantiomeric pair.* ***[Tl(dota)]⁻ does not react with Br^-, even when using an excess of the anion, but it forms a weak mixed complex with cyanide****. The dissociation of the* $[Tl(dota)]^-$ *complex was found to follow proton-assisted kinetics and to take place very slowly (~10 days), even in 1 M* $HClO_4$, *with the estimated half-life of the process being in the* 10^9 *h range at neutral pH. The solution dynamics of* $[Tl(dota)]^-$ *were investigated using* ^{13}C *NMR spectroscopy and DFT calculations. This dynamic behavior was attributed to the Λ(λλλλ) ↔ Δ(δδδδ) enantiomerization process, which involves both the inversion of the macrocyclic unit and the rotation of the pendant arms. According to our calculations, the arm-rotation process limits the Λ(λλλλ) ↔ Δ(δδδδ) interconversion.*

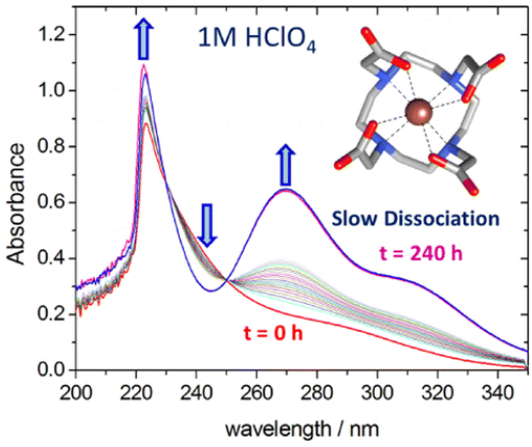

2.1.2. Experiments with Tl(III)-complexes of lower denticity ligands.

The results are summarized in Tamás Fodor's PhD thesis (Tamás Fodor's Thesis) and the BSc diploma work by Felicia Rozinka (Felícia Rozinka's diploma work) as follows:

Using ^{205}Tl-NMR spectra, the Tl(III)-complexes of hexadentate ligands CDTA-BBA and cisDO2A were shown to form mixed-ligand complexes with iodide ions, while the Tl(III)-complex of the heptadentate ligand DO3A does not. The stability constant of $[Tl(DO2A)]^+$ was determined by UV-Vis spectrophotometry, $\log K_{[Tl(DO2A)]}=41\pm3$, was found larger than that of $[Tl(EDTA)]^-$ ($\log K_{[Tl(EDTA)]}=37$), but smaller than the estimated stability of $[Tl(DOTA)]^-$. The equilibrium constants specific to the formation of Tl(III)L-OH mixed ligand complexes were determined by pH-potentiometry. Two equilibrium constants were calculated in case of all ligands. The stability constants of [Tl(CDTA-BBA)I] and [Tl(DO2A)I] mixed-ligand complexes are 5.79±0.54 and 4.13±0.08 respectively. Both complexes can be viewed as promising compounds for the binding of iodide and are worth future investigation.

2.1.3. ***Synthesis, Structure, and Antibacterial Activity of a Thallium(III)-Containing Polyoxometalate, $[Tl_2\{B\text{-}\beta\text{-}SiW_8O_{30}(OH)\}_2]^{12-}$*** in *Inorg. Chem.*, **2016**, *55*, 10118-10121.; https://doi.org/10.1021/acs.inorgchem.6b01921, and Tamás Fodor's Thesis

Note: The Bremen–group contacted us in 2014 during a COST meeting in Nürnberg, the Tl-POM system(s) fits very well to our work with robust Tl(III)-complexes, although it was not in the submitted proposal.

In solid $(NH_4)_5K_7[Tl_2\{B\text{-}\beta\text{-}SiW_8O_{30}(OH)\}_2]\cdot19H_2O$ the $[Tl_2\{B\text{-}\beta\text{-}SiW_8O_{30}(OH)\}_2]^{12-}$ architecture presents a polyanion with idealized C_{2h} symmetry, which consists of two thallium(III) centers and two $\{B\text{-}\beta\text{-}SiW_8O_{31}\}$ POM units. The two thallium(III) centers are both six-coordinated, and each thallium ion is coordinated to two $\{B\text{-}\beta\text{-}SiW_8O_{31}\}$ lacunary POM fragments via four terminal O atoms of the two complete tungsten-oxo triads and two terminal O atoms of two $\{SiO_4\}$ hetero groups. This

structure is fully retained in solution and contains two thallium centers within scalar coupling distance, as evidenced by ^{205} and ^{203} Tl NMR spectra. Both spectra appear as pseudo-triplets attributed to the spin-spin coupling between two sterically identical Tl-atoms. Further fine structure can be observed due to spin-spin coupling with ^{183}W atoms (14.3%). The two different values for $^{2}J(^{203}Tl\text{-}^{183}W)$ are ca. 470 and 350 Hz, respectively, and the corresponding values for $^{2}J(^{205}Tl\text{-}^{183}W)$ are ca 1% larger.

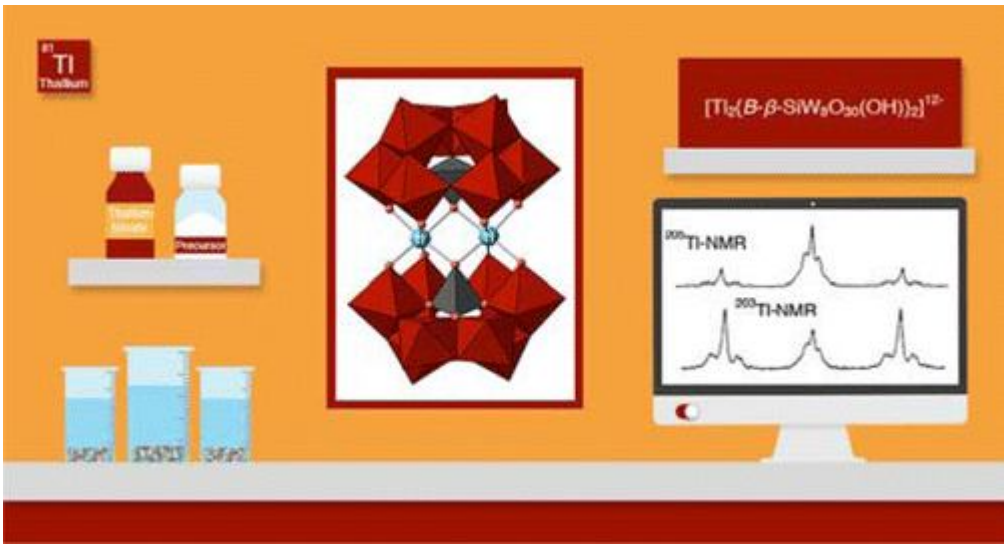

2.2. Mixed complexes with the "hard" Al(III) center

2.2.1. ***Equilibrium and dissociation kinetics of the [Al(NOTA)] complex (NOTA: 1,4,7-triazacyclononane-1,4,7-triacetate)*** in *React. Kinet. Mech. Cat.*, **2015**, *116*, 19–33.; https://doi.org/10.1007/s11144-015-0892-6

The slowly forming parent complex is very stable (lgK_{AlNOTA}= 17.9±0.1) and inert in acidic conditions. The extraordinary high stability of [Al(NOTA)] indicates a good matching of cavity size of the ligand and size of metal ion. The dissociation is somewhat faster in alkaline solutions. The ternary $[Al(NOTA)(F)]^-$ complex via direct reaction of [Al(NOTA)] and F^- cannot be detected. In solvent mixture (1:1 ethanol:water) and heating, the ternary complex was found to form quantitatively within 15 minutes.

2.2.2. Experiments with Al(III)-complexes of lower denticity ligands

Similarly to the Tl(III) mixed ligand complexes, the formation of $[Al(CDTA)F]^{2-}$ and [Al(CDTA-BBA)F] has been investigated. The stability and protonation constants of the $[Al(CDTA)]^-$ and $[Al(CDTA\text{-}BBA)]^+$ were determined by using pH-potentiometric methods while ^{19}F NMR was used to prove the formation of mixed fluoro complexes. The $[Al(CDTA)F]^{2-}$ complex was formed completely in 1 to 1 $[Al(CDTA)]^-$:F^- ratio in the mM concentration range. In the case of $[Al(CDTA\text{-}BBA)]^+$, the

F^- ion was found to compete with the CDTA-BBA ligand for Al(III), thus a part of the Al(III) ion was released forming AlF_x^{3-x} species. The rate of the F^- exchange between the free F^- and the [Al(CDTA-BBA)F] was also studied by magnetization transfer experiments. The system did not show any exchange process on the ^{19}F T_1 time scale. This is good news for PET application. As expected from the quadrupolar nature of the Al(III) ion, the T_1 longitudinal relaxation time of the coordinated F^- is 3-4 times shorter than the free ion's T_1. This complex may become useful in ^{19}F NMR imaging based on Al-mixed complexes.

3. Preparation and chemical characterization of highly stable and/or inert Ga(III) complexes formed with open chain and macrocyclic ligands

3.1. ***A shortcut to high-affinity Ga-68 and Cu-64 radiopharmaceuticals: one-pot click chemistry trimerisation on the TRAP platform*** in *Dalton Trans.*, **2015**, *44*, 11137-11146.;
https://doi.org/10.1039/c5dt00576k

The protocol for bio-orthogonal TRAP conjugation via Cu(I)- catalyzed Huisgen-cycloaddition of terminal azides and alkynes (CuAAC) was optimized, including a detailed investigation of kinetic properties of Cu(II)–TRAP complexes. TRAP building blocks for CuAAC, TRAP(alkyne)$_3$ and TRAP(azide)$_3$ were obtained by amide coupling of propargylamine/3-azidopropyl-1-amine, respectively. Dissociation of any Cu(II)–TRAP species was found to be independent on the nature or excess of a competing chelator, confirming a proton-driven two-step mechanism. The respective thermodynamic stability constants and dissociation rates show that the Cu(II) complex of the TRAP-conjugate possesses lower thermodynamic stability but higher kinetic inertness. An extrapolated dissociation half life of >100 h at 37 °C and pH 7 confirms the suitability of TRAP-bioconjugates for application in Cu-64 PET (cf. $t_{1/2}$(Cu-64) = 12.7 h). In conclusion, the kinetic inertness profile of Cu(II)–TRAP conjugates allows for simple Cu(II) removal after click functionalisation by means of transchelation, but also confirms their suitability for Cu-64-PET as demonstrated previously.

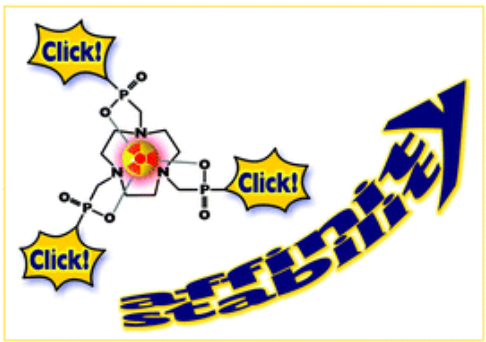

3.2. *Equilibrium, Kinetic and Structural Properties of Gallium(III) and Some Divalent Metal Complexes Formed with the New DATA^{m} and DATA^{5m} Ligands* in *Chem. Eur. J.*, **2017**, *23*, 10358 – 10371.; https://doi.org/10.1002/chem.201701508

The development of $^{68}Ge/^{68}Ga$ generators has made the positron-emitting ^{68}Ga isotope widely accessible and raised interest in new chelate complexes of Ga^{3+}. The hexadentate 1,4-di(acetate)-6-methyl[amino(methyl)acetate]- perhydro-1,4-diazepane (DATA^{m}) ligand and its bifunctional analogue, 1,4-di(acetate)-6-pentanoic acid[amino(methyl)acetate] perhydro-1,4-diazepane (DATA^{5m}), rapidly form complexes with ^{68}Ga in high radiochemical yield. The stability constants of DATA^{m} and DATA^{5m} complexes formed with Ga^{3+}, Zn^{2+}, Cu^{2+}, Mn^{2+} and Ca^{2+} have been determined by using pH potentiometry, spectrophotometry (Cu^{2+}) and ^{1}H and ^{71}Ga NMR spectroscopy (Ga^{3+}). The stability constants of Ga(DATA^{m}) and Ga(DATA^{5m}) complexes are slightly higher than those of Ga(AAZTA). The species distribution calculations indicated the predominance of Ga(L)OH mixed-hydroxo complexes at physiological pH. The ^{1}H and ^{71}Ga NMR spectroscopy studies provided information about the coordinated functional groups of ligands and on the kinetics of exchange between the Ga(L) and Ga(L)OH complexes. The transmetalation reactions between the Ga(L) complexes and Cu^{2+} citrate (6<pH<8.5) occur through both spontaneous and OH^{-}-assisted dissociation of the Ga(L)OH species. At pH 7.4 and 25°C, the half-lives of the dissociation of Ga(DATA^{m}), Ga(DATA^{5m}) and Ga(AAZTA) were 11, 44 and 24 h, respectively. Similar half-lives have been obtained for the ligand-exchange reactions between the Ga(L)OH complexes and transferrin. The equilibrium and kinetic data indicate that the Ga(DATA^{5m}) complex is a good ^{68}Ga-based radiodiagnostic candidate.

3.3. *Gallium(III) chelates of mixed phosphonate-carboxylate triazamacrocyclic ligands relevant to nuclear medicine: Structural, stability and in vivo studies* in *J. Inorg. Biochem.*, **2017**, *177*, 8-16.; https://doi.org/10.1016/j.jinorgbio.2017.08.015

Three triaza macrocyclic ligands, H_6NOTP (1,4,7-triazacyclononane-N,N',N''-trimethylene phosphonic acid), H_4NO2AP (1,4,7-triazacyclononane-N-methylenephosphonic acid-N',N''-dimethylenecarboxylic acid), and H_5NOA2P (1,4,7-triazacyclononane-N,N'-bis(methylenephosphonic acid)-N''-methylene carboxylic acid), and their gallium(III) chelates were studied in view of their potential interest as scintigraphic and PETimaging agents. A ^{1}H, ^{31}P and ^{71}Ga multinuclear NMR study gave an insight on the structure, internal dynamics and stability of the chelates in aqueous solution. In particular, the analysis of ^{71}Ga NMR spectra gave information on the symmetry of the Ga^{3+} coordination sphere and the stability of the chelates towards hydrolysis. The ^{31}P NMR spectra afforded information on the protonation of the non-coordinated oxygen atoms from the pendant phosphonate groups and on the number of species in solution. The ^{1}H NMR spectra allowed the analysis of the structure and the number of species in solution. ^{31}P and ^{1}H NMR titrations combined

with potentiometry afforded the measurement of the protonation constants ($logK_{Hi}$) and the microscopic protonation scheme of the triaza macrocyclic ligands. The remarkably high thermodynamic stability constant ($logK_{GaL}$=34.44(0.04) and stepwise protonation constants of $[Ga(NOA2P)]^{2-}$ were determined by potentiometry and ^{69}Ga and ^{31}P NMR titrations. Biodistribution and gamma imaging studies have been performed on Wistar rats using the radiolabeled $[^{67}Ga(NO2AP)]^{-}$ and $[^{67}Ga(NOA2P)]^{2-}$ chelates, having both demonstrated to have renal excretion. The correlation of the molecular properties of the chelates with their pharmacokinetic properties has been analysed.

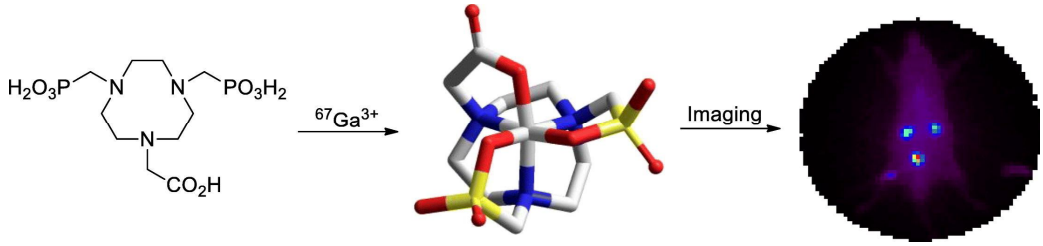

3.4. ***A rigidified AAZTA-like ligand as efficient chelator for ^{68}Ga radiopharmaceuticals*** in *ChemistrySelect*, **2016**, *2*, 163 –171., https://doi.org/10.1002/slct.201500051

The new cyclohexane-fused CyAAZTA ligand was synthesized to increase the structural rigidity of the heptadentate chelator AAZTA with the aim of improving the overall stability of its Ga^{III} complex. The stability constant of $Ga(CyAAZTA)^{-}$, determined both by pH-potentiometry ($logK_{GaL}$=21.39) and by ^{71}Ga NMR ($logK_{GaL}$=21.92), was found similar to that of GaAAZTA ($logK_{GaL}$=22.18). The kinetic inertness of $Ga(CyAAZTA)^{-}$ was investigated by following its transmetallation and ligand exchange reactions with Cu^{2+} and human serum transferrin, respectively. The formation of a hydroxido-complex near pH 7 decreases the half-life ($t_{1/2}$) of the dissociation reactions for $Ga(CyAAZTA)^{-}$ compared to $Ga(AAZTA)^{-}$ (8.5 h vs 21 h, pH 7.4). However, at pH < 7 the $t_{1/2}$ of $Ga(CyAAZTA)^{-}$ is much longer (234 h at pH 6). Finally, CyAAZTA was successfully radiolabelled with ^{68}Ga in acetate buffer at pH 3.8, in 15 minutes at room temperature at [CyAAZTA]=10 μM, with a labelling yield higher than 80 %. A 1 μM solution of CyAAZTA was successfully labelled (L.Y.: 97.4 %) in 5 minutes at 90 °C. Stability tests in human serum and in the presence of 50 mM DTPA showed no significant decomposition of $^{68}GaCyAAZTA$ over 90 minutes.

3.5. Study of the formation kinetics of $[Ga(DOTA)]^{-}$

Publication on the formation kinetics in water-ethanol mixture is in progress, the manuscript is in the hands of our German partners in Mainz. They have performed large scale labeling experiments with radiotracers. We performed the mechanistic study. The substantial increase in the reaction rate in

mixed solvents can be correlated to the different protonation ability of the free ligand and the H_2GaDOTA intermediate compared to those obtained in pure water.

4. Preparation of highly stable and/or inert Cu(II) complexes formed with (bifunctional) macrocyclic ligands

4.1. ***H_4octapa: Highly Stable Complexation of Lanthanide(III) Ions and Copper(II)*** in *Inorg. Chem.*, **2015**, *54*, 2345–2356., https://doi.org/10.1021/ic502966m

The acyclic ligand octapa^{4-} (H_4octapa = 6,6'-((ethane-1,2- diylbis((carboxymethyl)azanediyl)) bis(methylene))dipicolinic acid) forms stable complexes with the Ln^{3+} ions in aqueous solution. The stability constants determined for the complexes with La^{3+}, Gd^{3+}, and Lu^{3+} using relaxometric methods are $logK_{LaL}$=20.13(7), $logK_{GdL}$=20.23(4), and $logK_{LuL}$=20.49(5) (I=0.15 M NaCl). High stability constants were also determined for the complexes formed with divalent metal ions such as Zn^{2+} and ***Cu^{2+}*** *($logK_{ZnL}$=18.91(3) and $logK_{CuL}$=22.08(2)). UV–visible and NMR spectroscopic studies and density functional theory (DFT) calculations point to hexadentate binding of the ligand to Zn^{2+} and Cu^{2+}, the donor atoms of the acetate groups of the ligand remaining uncoordinated. The complexes formed with the Ln^{3+} ions are nine-coordinated thanks to the octadentate binding of the ligand and the presence of a coordinated water molecule. The stability constants of the complexes formed with the Ln^{3+} ions do not change significantly across the lanthanide series. A DFT investigation shows that this is the result of a subtle balance between the increased binding energies across the 4f period, which contribute to an increasing complex stability, and the parallel increase of the absolute values of the hydration free energies of the Ln^{3+} ions. In the case of the [Ln(octapa)(H_2O)]$^-$ complexes the interaction between the amine nitrogen atoms of the ligand and the Ln^{3+} ions is weakened along the lanthanide series, and therefore the increased electrostatic interaction does not overcome the increasing hydration energies. A detailed kinetic study of the dissociation of the [Gd(octapa)(H_2O)]$^-$ complex in the presence of* ***Cu^{2+}*** *shows that the metal-assisted pathway is the main responsible for complex dissociation at pH 7.4 and physiological [Cu^{2+}] concentration (1 μM)*

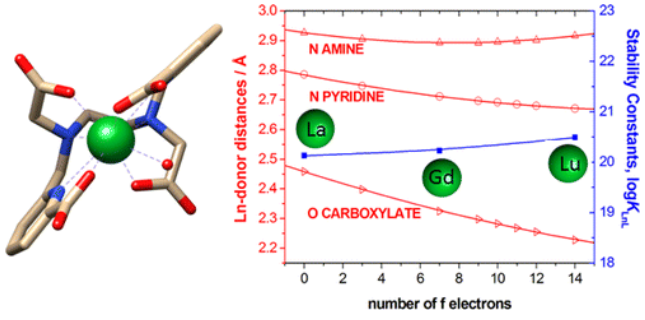

4.2. ***Highly Stable Complexes of Divalent Metal Ions (Mg^{2+}, Ca^{2+}, Cu^{2+}, Zn^{2+}, Cd^{2+}, and Pb^{2+}) with a Dota-Like Ligand Containing a Picolinate Pendant*** in *Eur. J. Inorg. Chem,*, **2014**, *36*, 6165–6173., https://doi.org/10.1002/ejic.201402693

*The stability constants of complexes of the macrocyclic ligand do3a-pic^{4-} (H_4do3a-pic=2,2',2''-{10-[(6-carboxypyridin-2-yl)methyl]-1,4,7,10-tetraazacyclododecane-1,4,7-triyl}triacetic acid) with several divalent metal ions (Pb^{2+}, Cd^{2+}, Zn^{2+}, **Cu^{2+}**, Ca^{2+}, and Mg^{2+}) have been determined by using pH-potentiometric titrations (I=0.1 M KCl, 25 °C). The stability of these complexes follows the trend **Cu^{2+}** > $Cd^{2+} \approx Pb^{2+} \approx Zn^{2+} >> Ca^{2+} >> Mg^{2+}$. A particularly high stability constant has been determined for the **Cu^{2+} complex [logK_{CuL}=23.20(4)].** Analysis of the titration curves indicate the presence of protonated forms of the complexes in solution, with protonation constants of log$K_{M(HxL)}$=6.9–2.0 (x=1, 2, or 3). The structure of the complexes in solution has been investigated by using ^{1}H and ^{13}C NMR spectroscopy and DFT calculations performed in aqueous solution at the TPSSh/6-31G(d) level. In the case of the Pb^{2+} and Cd^{2+} complexes, relativistic effects were considered with the use of relativistic effective core potentials. Calculations show that the complexes with the largest metal ions (Pb^{2+} and Ca^{2+}) are nine-coordinate, with their coordination polyhedra being best described as capped twisted square antiprisms. The Cd^{2+} and Mg^{2+} complexes are seven-coordinate, with the metal ions being bound to the four nitrogen atoms of the cyclen unit and the three acetate pendant arms. Finally, in the **Cu^{2+}** and Zn^{2+} complexes, the metal ions are six-coordinated, with the metal ions being asymmetrically placed inside the macrocyclic cavity of the ligand, and the coordination polyhedra can be described as an octahedron and a trigonal prism, respectively.*

4.3. see 3.1.

4.4. ***Solution Structures, Stabilities, Kinetics, and Dynamics of DO3A and DO3A–Sulphonamide Complexes*** in *Inorg. Chem.*, **2014**, *53*, 2858–2872.; https://doi.org/10.1021/ic4025958

*The stability constants of the DO3A−SA and DO3A complexes formed with Mg^{2+}, Ca^{2+}, Mn^{2+}, Zn^{2+}, and **Cu^{2+} ions** are similar, whereas the logK_{LnL} values of [Ln(DO3A−SA)]$^{-}$ complexes are 2 orders of magnitude higher than those of the [Ln(DO3A)] complexes. The logK_{LnHL} values of the [Ln(DO3A−SA)]$^{-}$ complexes are lower by about 4 logK units, indicating a strong interaction between the Ln^{3+} ions and the sulphonamide N atom. The [Ln(HDO3A−SA)] complexes are formed via triprotonated *[Ln(H_3DO3A−SA)]$^{2+}$ intermediates which rearrange to the final complex in an OH^{-}-assisted deprotonation process. **The transmetalation reaction of [Gd(HDO3A−SA)] with Cu^{2+} is very slow ($t_{1/2}$ = 5.6 × 10^3 h at pH = 7.4), and it mainly occurs through proton-assisted dissociation of the complex.** The fast isomerization and the lower activation parameters of [Ln(DO3A−SA)]$^{-}$ have been*

confirmed by theoretical calculations in vacuo and by using the polarizable continuum model. ***The solid state X-ray structure of [Cu(H$_2$DO3A−SA)] shows distorted octahedral coordination.***

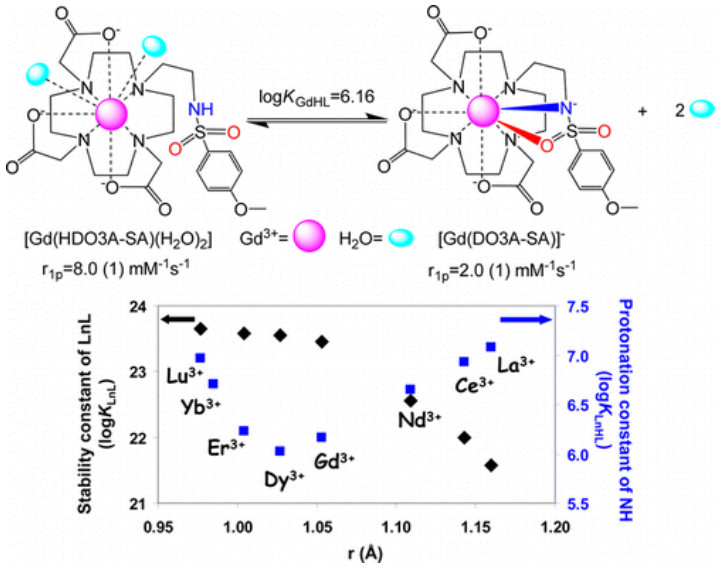

4.5. ***A Pyridine-Based Ligand with Two Hydrazine Functions for Lanthanide Chelation: Remarkable Kinetic Inertness for a Linear, Bishydrated Complex*** in *Inorg. Chem.*, **2015**, *54*, 5991–6003.; https://doi.org/10.1021/acs.inorgchem.5b00804

To study the influence of hydrazine functions in the ligand skeleton, we designed the heptadentate HYD ligand (2,2',2",2"'-(2,2'-(pyridine-2,6-diyl)bis(2-methylhydrazine-2,1,1-triyl)) tetraacetic acid) and compared the thermodynamic, kinetic, and relaxation properties of its Ln^{3+} complexes to those of the parent pyridine (Py) analogues without hydrazine (Py=2,6-pyridinebis(methanamine)-N,N,N',N'-tetraacetic acid). Thermodynamic stability constants have been obtained by pH-potentiometry and UV–visible spectrophotometry for various Ln^{3+} and physiological cations (Zn^{2+}, Ca^{2+}, ***Cu^{2+}****). LnHYD stability constants show the same trend as those of LnDTPA complexes along the Ln^{3+} series, with logK=18.33 for Gd^{3+}, comparable to the Py analogue.* ***CuHYD has a particularly high stability (logK>19)*** *preventing its determination from pH-potentiometric measurements.* ***The stability constant of CuPy was also revisited and found to be underestimated in previous studies, highlighting that UV–visible spectrophotometry is often indispensable to obtain reliable stability constants for Cu^{2+} chelates.*** *The dissociation of GdL, assessed by studying the Cu^{2+}-exchange reaction, occurs mainly via an acid-catalyzed process, with limited contribution from direct Cu^{2+} attack. The kinetic inertness of GdHYD is remarkable for a linear bishydrated chelate; the 25-fold increase in the dissociation half-life with respect to the monohydrated commercial contrast agent GdDTPA (t$_{1/2}$=5298 h for GdHYD vs 202 h for GdDTPA) is related to the rigidity of the HYD ligand due to the pyridine and methylated hydrazine functions of the backbone. A combined analysis of variable-temperature ^{17}O NMR and NMRD data on GdHYD yielded the microscopic parameters influencing relaxation properties. The*

high relaxivity (r_1=7.7 mM^{-1} s^{-1} at 20 MHz, 25 °C) results from the bishydrated character of the complex combined with an optimized water exchange rate (k_{ex}^{298}=7.8×10^6 s^{-1}). The two inner-sphere water molecules are not replaced through interaction with biological cations such as carbonate, citrate, and phosphate as monitored by ^{1}H relaxivity and luminescence lifetime measurements.

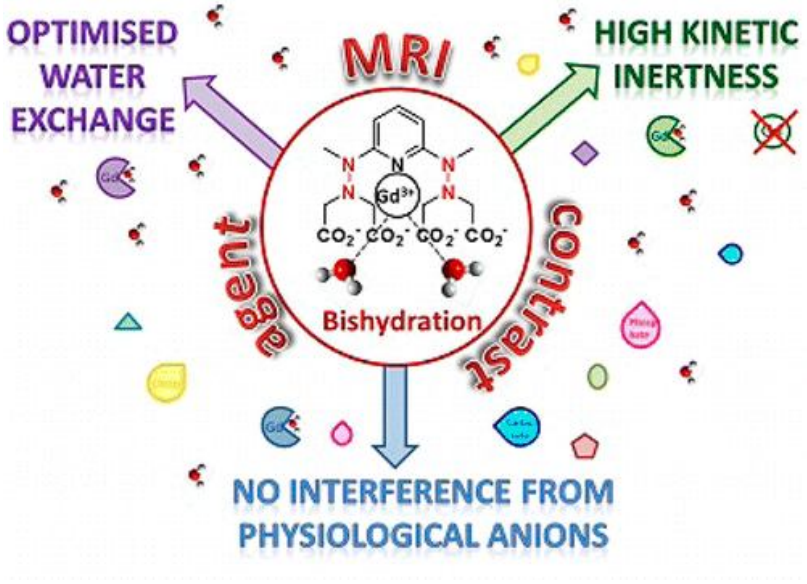

4.6. ***High kinetic inertness of a bis-hydrated Gd-complex with a constrained AAZTA-like ligand*** in *Chem. Commun.*, **2016**, *52*, 11235-11238.;
https://doi.org/10.1039/C6CC04753J

*Kinetic inertness is a key property for a Gd-based contrast agent. The Gd^{III} complex of a cyclohexyl-fused AAZTA derivative shows the highest kinetic inertness for non-macrocyclic bis hydrated (*q=*2) Gd^{III}-complexes with a dissociation half-life of 91 years under physiological conditions, very close to that of macrocyclic clinically approved contrast agents. It also shows optimal relaxometric performance (r_1=8.3 mM^{-1} s^{-1} at 20 MHz and 25 °C) due to the presence of two inner sphere water molecules in fast exchange with bulk water and not displaced by endogenous anions.*

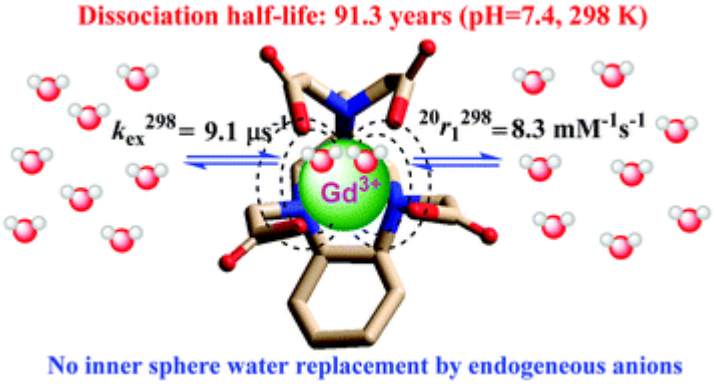

Note: Inertness was studied via metall exchange reaction with Cu(II). The inertness of the bis-hydrated complex is remarkable for ligand design.

5. Microwave activation of complex formation reactions

5.1. ***Lanthanide(III) Complexes with a Reinforced Cyclam Ligand Show Unprecedented Kinetic Inertness***" in *J. Am. Chem. Soc.*, 2014, 136 (52), pp 17954–17957., https://doi.org/10.1021/ja511331n

Lanthanide(III) complexes of a cross-bridged cyclam derivative containing two picolinate pendant arms are kinetically inert in very harsh conditions such as 2 M HCl, with no dissociation being observed for at least 5 months. Importantly, the [Ln(dota)]$^-$ complexes, which are recognized to be extremely inert, dissociate under these conditions with lifetimes in the range ca. 1 min to 12 h depending upon the Ln^{3+} ion. X-ray diffraction studies reveal octadentate binding of the ligand to the metal ion in the [Eu(cb-tedpa)]$^+$ complex, while ^1H and ^{13}C NMR experiments in D_2O point to the presence of a single diastereoisomer in solution with a very rigid structure. The structure of the complexes in the solid state is retained in solution, as demonstrated by the analysis of the Yb^{3+}-induced paramagnetic shifts.

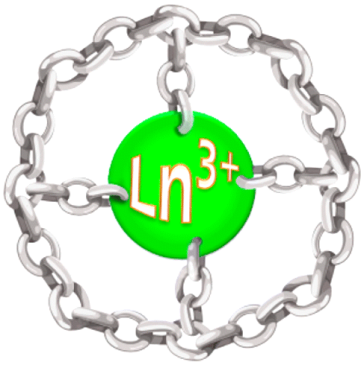

The relevance of microwave activation is described in the paper as follows:

Ln^{3+} complexes of cb-tedpa appears to be rather slow, and requires the use of a solvent with a high boiling point and long reaction times (ca. 7 days). However, the yields obtained were rather low (ca. 24%). To overcome this, the synthesis of the Eu^{3+} complex was carried out under microwave radiation (150 ºC, 250 psi, maximum power 300 W) in n-butanol using DIPEA as a base and a 100% excess of $EuCl_3 \cdot 6H_2O$. The formation of the complex was quantitative after 8 h, as demonstrated by NMR spectroscopy.

6. Mechanistic and structural studies by theoretical calculations. Developing new computer program for equilibrium studies

6.1. High level DFT calculations were used and published in several papers (see 1.2.1., 1.2.3., 2.1.1., 4.1., 4.2., 5.1., 8.4.). The calculations were dominantly carried out by Carlos Platas Iglesias in La Coruna, but the valuable results on Tl(III)DOTA system were contributed by M. Purgel working in Debrecen.

6.2. Developing a new version of the PSEQUAD program.

The new version of the computer program for evaluation of equilibrium constants uses Windows with support of Matlab. The program uses Excel files and graphics of Windows instead of text files. The new version has been successfully tested in our lab, and we use it with the free version Matlab also.

7. Radiochemical studies

7.1. ***AAZTA: An Ideal Chelating Agent for the Development of ^{44}Sc PET Imaging Agents*** in *Angew. Chem. Int. Ed.*, **2017**, *56*, 2118 –2122., https://doi.org/10.1002/anie.201611207

Unprecedented fast and efficient complexation of Sc(III) was demonstrated with the chelating agent AAZTA (AAZTA=1,4-bis(carboxymethyl)-6-[bis(carboxymethyl)]amino-6-methylperhydro-1,4-diazepine) under mild experimental conditions. The robustness of the ^{44}Sc(AAZTA)$^{-}$ chelate and conjugated biomolecules thereof is further shown by in vivo PET imaging in healthy and tumor mice models. The new results pave the way towards development of efficient Sc-based radiopharmaceuticals using the AAZTA chelator.

7.2 see **3.3.**

7.3. see **3.4.**

8. Related Miscellaneous systems

8.1. ***The Role of Equilibrium and Kinetic Properties in the Dissociation of Gd[DTPA-bis(methylamide)] (Omniscan) at near to Physiological Conditions*** in *Chem. Eur. J.,* 2015, 21, 4789-4799., https://doi.org/10.1002/chem.201405967

[Gd(DTPA-BMA)] is the principal constituent of Omniscan, a magnetic resonance imaging (MRI) contrast agent. In body fluids, endogenous ions (Zn^{2+}, Cu^{2+}, and Ca^{2+}) may displace the Gd^{3+}. To assess the extent of displacement at equilibrium, the stability constants of DTPA-BMA^{3-} complexes of Gd^{3+}, Ca^{2+}, Zn^{2+}, and Cu^{2+} have been determined at 37 °C in 0.15 M NaCl. The order of these stability constants is as follows: GdL≈CuL>ZnL ≫CaL. Applying a simplified blood plasma model, the extent of dissociation of Omniscan (0.35 mM [Gd(DTPA-BMA)]) was found to be 17 % by the formation of $Gd(PO_4)$, $[Zn(DTPA\text{-}BMA)]^-$ (2.4 %), $[Cu(DTPA\text{-}BMA)]^-$ (0.2 %), and $[Ca(DTPA\text{-}BMA)]^-$ (17.7 %). By capillary electrophoresis, the formation of $[Ca(DTPA\text{-}BMA)]^-$ has been detected in human serum spiked with [Gd(DTPA-BMA)] (2.0 mM) at pH 7.4. Transmetallation reactions between [Gd(DTPA-BMA)] and Cu^{2+} at 37 °C in the presence of citrate, phosphate, and bicarbonate ions occur by dissociation of the complex assisted by the endogenous ligands. At physiological concentrations of citrate, phosphate, and bicarbonate ions, the half-life of dissociation of [Gd(DTPA-BMA)] was calculated to be 9.3 h at pH 7.4. Considering the rates of distribution and dissociation of [Gd(DTPA-BMA)] in the extracellular space of the body, an open two-compartment model has been developed, which allows prediction of the extent of dissociation of the Gd^{III} complex in body fluids depending on the rate of elimination of the contrast agent.

Note: The publication focuses on Omniscan, which was used in most of the detected NSF cases. However, we are going to use the same methodology for our newly developed metal-complexes for any different image-modalities (e.g. MRI, SPECT, PET or theragnostics).

8.2. ***Thermodynamic stability, kinetic inertness and relaxometric properties of monoamide derivatives of lanthanide(III) DOTA complexes*** in *Dalton Trans.*, **2015**, *44*, 5467-5478.; https://doi.org/10.1039/C4DT03939D

A complete thermodynamic and kinetic solution study on lanthanide(III) complexes with monoacetamide (DOTAMA, L_1) and monopropionamide (DOTAMAP, L2) derivatives of DOTA (DOTA = 1,4,7,10-tetraazacyclododecane- 1,4,7,10-tetraacetic acid) was undertaken with the aim to elucidate their stability and inertness in aqueous media. The stability constants of GdL1 and GdL2 are comparable, whereas a more marked difference is found in the kinetic inertness of the two complexes.
A novel DOTAMAP-based bifunctional chelating ligand and its deoxycholic acid derivative (L5) were also synthesized. The relaxometric properties of the supramolecular adduct of GdL5 with human serum albumin (HSA) were investigated The Gd(III) complexes with DOTAMAP macrocyclic ligands can represent good candidates for stable and highly effective bioconjugate systems for molecular imaging applications.

Note: The increased inertness of the LnL_2-complex might be retained in other complexes including Mn-MC-monoamide derivatives, helping the fine-tuning of our Mn-binder ligands. Experiments are in progress in that direction.

8.3. ***Definition of the Labile Capping Bond Effect in Lanthanide Complexes*** in *Chem. Eur. J.*, **2017**, *23*, 1110–1117.; https://doi.org/10.1002/chem.201604390

We report two novel macrocyclic ligands containing a cyclen unit, a methyl group, a picolinate arm and two acetate pendant arms attached to two nitrogen atoms of the macrocycle either in trans (1,7-H_3Medo2ampa) or in cis (1,4-H_3Medo2ampa) positions. These ligands provide eight-coordination to the Ln^{3+} ions leaving a coordination position available for a water molecule that occupies a capping position in the twisted square antiprismatic polyhedron (1,4-H_3Medo2ampa) or one of the positions of the square antiprism (1,7-H_3Medo2ampa). The charge neutral [Gd(1,7-Medo2ampa)] complex presents an unprecedentedly low water exchange rate ($k_{ex}^{298}=8.8x10^3$ s^{-1}), while water exchange in [Gd(1,4-Medo2ampa)] is three orders of magnitude faster ($k_{ex}^{298}=6.6x10^6$ s^{-1}). These results showcase the labile capping bond phenomenon: a ligand occupying a capping position is hindered by the environment and thus is intrinsically labile.

8.4. ***Complexation of Ln^{3+} Ions with Cyclam Dipicolinates: A Small Bridge that Makes Huge Differences in Structure, Equilibrium, and Kinetic Properties*** in *Inorg. Chem.*, **2016**, *55*, 2227–2239.; https://doi.org/10.1021/acs.inorgchem.5b02627

The coordination properties toward the lanthanide ions of two macrocyclic ligands based on a cyclam platform containing picolinate pendant arms have been investigated. The synthesis of the ligands was achieved by using the well-known bis-aminal chemistry. One of the cyclam derivatives (cb-tedpa^{2-}) is reinforced with a cross-bridge unit, which results in exceptionally inert $[Ln(cb\text{-}tedpa)]^+$ complexes. The X-ray structures of the [La(cb-tedpa)Cl], $[Gd(cb\text{-}tedpa)]^+$, and $[Lu(Me_2tedpa)]^+$ complexes indicate octadentate binding of the ligands to the metal ions. The analysis of the Yb^{3+}-induced shifts in $[Yb(Me_2tedpa)]^+$ indicates that this complex presents a solution structure very similar to that observed in the solid state for the Lu^{3+} analogue. The X-ray structures of $[La(H_2Me_2tedpa)_2]^{3+}$ and $[Yb(H_2Me_2tedpa)_2]^{3+}$ complexes confirm the exocyclic coordination of the metal ions, which gives rise to coordination polymers with the metal coordination environment being fulfilled by oxygen atoms of the picolinate groups and water molecules. The X-ray structure of $[Gd(Hcb\text{-}tedpa)_2]^+$ also indicates exocyclic coordination that in this case results in a discrete structure with an eight-coordinated metal ion. The nonreinforced complexes $[Ln(Me_2tedpa)]^+$ were prepared and isolated as chloride salts in nonaqueous media. However, these complexes were found to undergo dissociation in aqueous solution, except in the case of the complexes with the smallest Ln^{3+} ions (Ln^{3+} = Yb^{3+} and Lu^{3+}). A

DFT investigation shows that the increased stability of the [Ln(Me$_2$tedpa)]$^+$ complexes in solution across the lanthanide series is the result of an increased binding energy of the ligand due to the increased charge density of the Ln^{3+} ion.

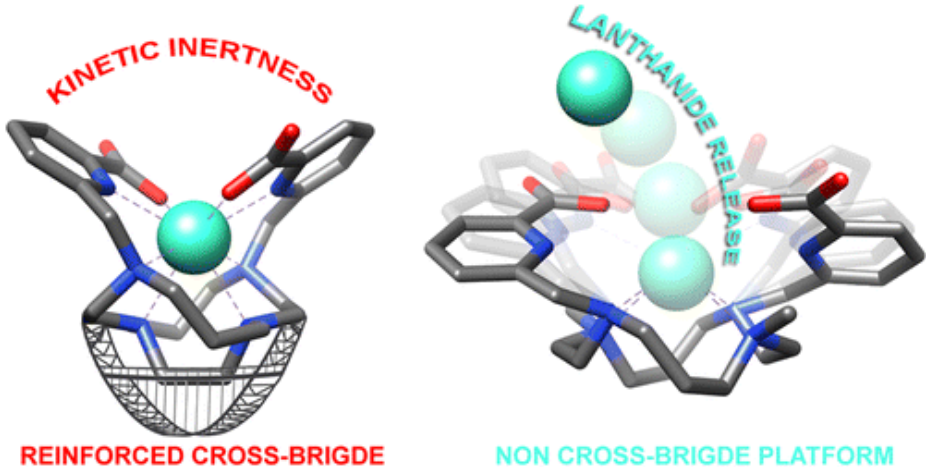

Note: The relevance to Mn(II)-complexes is that the inertness of the non-bridged complexes is very sensitive to the size of the metal ions, i.e. this platform is not a promising one.

8.5. ***Approaching the Kinetic Inertness of Macrocyclic Gadolinium(III)- Based MRI Contrast Agents with Highly Rigid Open-Chain Derivatives***, in *Chem. Eur. J.,* **2016**, *22*, 896–901.; https://doi.org/10.1002/chem.201503836

A highly rigid open-chain octadentate ligand (H$_4$cddadpa) containing a diaminocylohexane unit to replace the ethylenediamine bridge of 6,6'-[(ethane-1,2 diylbis{(carboxymethyl)azanediyl})bis(methylene)]dipicolinic acid (H$_4$octapa) was synthesized. This structural modification improves the thermodynamic stability of the Gd^{3+} complex slightly (log K$_{GdL}$=20.68 vs. 20.23 for [Gd(octapa)]$^-$) while other MRI-relevant parameters remain unaffected (one coordinated water molecule; relaxivity r$_1$=5.73 mm^{-1} s^{-1} at 20 MHz and 295 K). Kinetic inertness is improved by the rigidifying effect of the diaminocylohexane unit in the ligand skeleton (half-life of dissociation for physiological conditions is 6 orders of magnitude higher for [Gd(cddadpa)]$^-$ (t$_{1/2}$=1.49×10^5 h) than for [Gd(octapa)]$^-$. The kinetic inertness of this novel chelate is superior by 2–3 orders of magnitude compared to non-macrocyclic MRI contrast agents approved for clinical use.

8.6. ***Nyíltláncú és makrociklusos aminokarboxilát ligandumok szintézise és fémkomplexeik vizsgálata: koordinációskémia az orvosi képalkotás szolgálatában (Synthesis of Linear and Macrocyclic Aminopolycarboxylate Ligands and Chemical Characterization of their Metal***

Complexes for Safe Use in Medical Imaging), *MAGYAR KÉMIAI FOLYÓIRAT - KÉMIAI KÖZLEMÉNYEK*, 2017, 123, 82-93., https://doi.org/10.24100/MKF.2017.02.82

This invited paper is written in Hungarian summarising our results from the last decade including a sketchy overview of the reported project here. We hope that this review increases the visibility of our group inside the Hungarian scientific community.

Abbreviations:

MRI: Magnetic Resonance Imaging

PET: Positron Emission Tomography

SPECT: Single Photon Emission Computed Tomography

NMR: Nuclear Magnetic Resonance

DFT: Density functional theory

NMRD: Nuclear Magnetic Relaxation Dispersion

HSA: Human Serum Albumin

Structures of the ligands mentioned in the text:

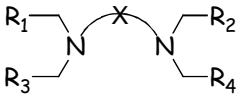

EDTA (R_1=R_2=R_3=R_4=CH_2-CO_2H, X=CH_2-CH_2)
CDTA (R_1=R_2=R_3=R_4=CH_2-CO_2H, X=1,2-cyclohexyl)
PhDTA (R_1=R_2=R_3=R_4=CH_2-CO_2H, X=1,2-phenyl)
BDTA (R_1=R_2=R_3=R_4=CH_2-CO_2H, X=-$(CH_2)_4$-)
octapa (R_1=R_2=CH_2-CO_2H, R_3=R_4=PIC*, X=CH_2-CH_2)
cddadpa (R_1=R_2=CH_2-CO_2H, R_3=R_4=PIC*, X=1,2-cyclohexyl)
CDTA-BBA (R_1=R_2=CH_2-CO_2H, R_3=R_4=CH_2-CO-NH-$(CH_2)_3$-CH_3 X=1,2-cyclohexyl)

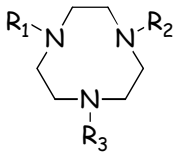

NOTA (R_1=R_2=R_3=CH_2-CO_2H)
TRAP (R_1=R_2=R_3=CH_2-PO_2-R)
NOTP (R_1=R_2=R_3=CH_2-PO_3H_2)
NO2AP (R_1=R_2=CH_2-CO_2H, R_3=CH_2-PO_3H_2)
NOA2P (R_1=CH_2-CO_2H, R_2=R_3=CH_2-PO_3H_2)
NOMPA (R_1=R_2=H, R_3=PIC*)

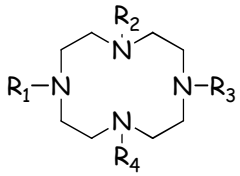

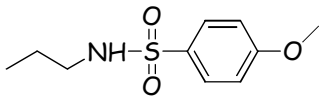

SA*

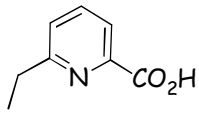

PIC*

DOTA (R_1=R_2=R_3=R_4=CH_2-CO_2H)
DO3A (R_1=R_2=R_3=CH_2-CO_2H, R_4=H)
cis-DO2A (R_1=R_2=CH_2-CO_2H, R_3=R_4=H)
trans-DO2A (R_1=R_3=CH_2-CO_2H, R_2=R_4=H)
dodpa (R_1=R_3=H, R_2=R_4=PIC*)
Me_2dodpa (R_1=R_3=CH_3, R_2=R_4=PIC*)
1,4-DO2AM (R_1=R_2=H, R_3=R_4=CH_2-CO-N$(CH_3)_2$)
DO3A-PIC or do3ampa (R_1=R_2=R_3=CH_2-CO_2H, R_4=PIC*)
DOTAMA (R_1=R_2=R_3=CH_2-CO_2H, R_4=CH_2-CO-NH-$(CH_2)_2$-NH_2)
DOTAMAP (R_1=R_2=R_3=CH_2-CO_2H, R_4=$(CH_2)_2$-CO-NH-$(CH_2)_2$-NH_2)
1,7-Medo2ampa (R_1=R_3=CH_3, R_2=R_4=PIC*)
1,4-Medo2ampa (R_1=R_2=CH_3, R_3=R_4=PIC*)
DO3A-SA (R_1=R_2=R_3=CH_2-CO_2H, R_4=SA*)
dompa (R_1=R_2=R_3=H, R_4=PIC*)

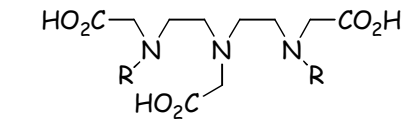

DTPA (R=CH_2-CO_2H)
DTPA-BMA (R=CH_2-$CONHCH_3$)

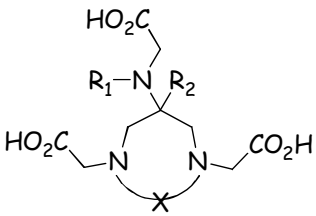

AAZTA (R_1=CH_2-CO_2H, R_2=CH_3, X=CH_2-CH_2)
CyAAZTA (R_1=CH_2-CO_2H, R_2=CH_3, X=1,2-cyclohexyl)
$DATA^m$ (R_1=R_2=CH_3, X=CH_2-CH_2)
$DATA^{5m}$ (R_1=CH_3, R_2=$(CH_2)_4$-CO_2H, X=CH_2-CH_2)

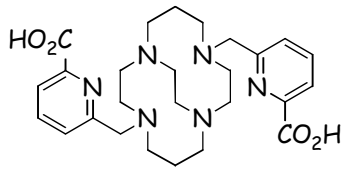

CB-TEDPA

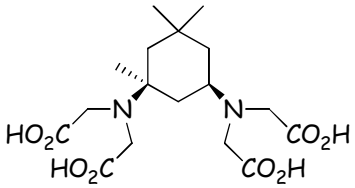

cis-IPDTA

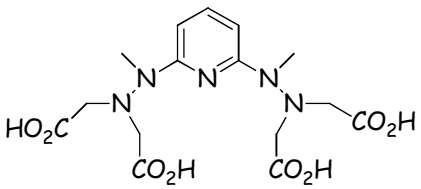

HYD

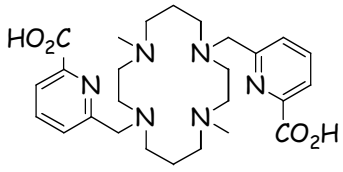

Me2TEDPA

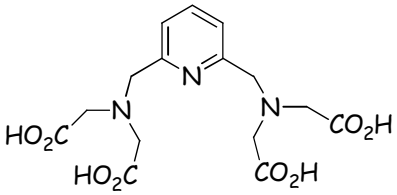

Py